Naunyn-Schmiedeberg's Arch Pharmacol (2009) 379:11–26
DOI 10.1007/s00210-008-0345-0

ORIGINAL ARTICLE

A novel screening strategy to identify ABCB1 substrates and inhibitors

Oliver von Richter · Hristos Glavinas · Peter Krajcsi · Stephanie Liehner · Beate Siewert · Karl Zech

Received: 15 February 2008 / Accepted: 4 August 2008 / Published online: 29 August 2008

Abstract We tested the hypothesis whether data on ABCB1 ATPase activity and passive permeability can be used in combination to identify ABCB1 substrates and inhibitors. We determined passive permeability using an artificial membrane permeability assay (HDM-PAMPA) and ABCB1 function, i.e., vanadate-sensitive ATPase activity for a training set (40 INN drugs) and a validation set (26 development compounds). In parallel experiments, we determined ABCB1 function, i.e., vectorial transport in a Caco-2 cell monolayer, and ABCB1 inhibition, i.e., calcein AM extrusion out of K562-MDR cells, to cross-validate the results with cellular assays. We found that compounds that did not modulate ABCB1-ATPase did also not affect calcein AM extrusion and were not actively transported by ABCB1 in Caco-2 cell monolayers. The results corroborated the effect of passive permeability as an important covariate of active transport: active transport in Caco-2 monolayer was only apparent for compounds showing low passive permeability (<5.0 $cm \times 10^{-6}/s$) in the HDM-PAMPA assay whereas compounds with high passive permeability (>50 $cm \times 10^{-6}/s$) were shown to inhibit calcein AM efflux with IC_{50} values close to their respective K_m value obtained for ABCB1-ATPase. The use of HDM-PAMPA in combination with ABCB1-ATPase offers a simple, inexpensive experimental approach capable of identifying ABCB1 inhibitors as well as transported substrates.

Keywords ABCB1 · P-glycoprotein · Drug transport · ATPase · PAMPA · Passive permeability

Abbreviations

Calcein AM	calcein acetoxymethylester
DMSO	dimethyl sulfoxide
DMEM	Dulbecco's modified Eagle's medium
INN	international nomenclature name
HBSS	Hanks' balanced salt solution
HPLC	high-performance liquid chromatography
GF120918	GG918 elacridar
LLOQ	lower limit of quantification
MDCK	Madin–Darby canine kidney cells

Introduction

ABCB1, also known as P-glycoprotein, the product of the multidrug resistance 1 (*MDR1*) gene, translocates a broad variety of xenobiotics out of cells. ABCB1 is assumed to be one of the most important transporters for drug disposition in humans (for review, see Fromm 2004 and Petzinger et al. 2006). ABCB1 functions in three main ways: it limits drug entry into the body after oral drug administration as a result of its expression in the luminal (apical) membrane of enterocytes (Greiner et al. 1999). Once the drug has reached the blood circulation, ABCB1 promotes drug elimination into the bile (Drescher et al. 2003) and urine as a result of its expression in the canalicular membrane of hepatocytes

O. von Richter · S. Liehner · B. Siewert · K. Zech
Division of Drug Metabolism and Pharmacokinetics,
Altana Pharma AG,
Konstanz, Germany

H. Glavinas · P. Krajcsi
Division R&D, Solvo Biotechnology,
Budaörs 2040, Hungary

O. von Richter (✉)
Department of Pharmacokinetics and Pharmacometrics,
AiCuris GmbH & Co KG,
Friedrich-Ebert-Str. 475,
Wuppertal 42117, Germany
e-mail: oliver.von.richter@aicuris.com

(Thiebaut et al. 1987) and in the luminal membrane of proximal tubule cells in the kidneys, respectively. In addition, once a xenobiotic has reached the systemic blood circulation, ABCB1 limits drug penetration into sensitive tissues, e.g., into the brain (Cordon-Cardo et al. 1989), heart (Meissner et al. 2002), testes (Choo et al. 2000), lymphocytes (Klimecki et al. 1994), and fetal circulation (Smit et al. 1999). Acting alone or in concert with drug-metabolizing enzymes, ABCB1 can affect the pharmacokinetics and pharmacodynamics of its substrates (Cummins et al. 2002).

ABCB1 belongs to the adenosine triphosphate (ATP)-binding cassette (ABC) transporter superfamily using ATP as its energy source. Most individual ABC transporters display tightly restricted substrate specificity related to their physiological function. Mammalian ABCB1, however, is able to interact with a large number of structurally unrelated drugs (Litman et al. 1997b). Recent investigations suggest that this is due to ABCB1 containing a minimum of four binding sites rather than a single site of broad substrate specificity, which display complex allosteric interactions (Martin et al. 2000). Furthermore, ABCB1 substrates reside in the plasma membrane and, in consequence, the rate and the extent at which the substrate-binding site is reached, i.e., passive permeability, has to be taken into account when analyzing ABCB1-mediated transport (Bentz et al. 2005). Taken together, the identification of ABCB1 substrates and inhibitors is difficult due to the functional complexity of the transporter and the influence of passive permeability on ABCB1 kinetics.

This is reflected by the large number of in vitro assays available to determine the interactions of molecules with ABCB1 (for review, see Glavinas et al. 2004), often yielding conflicting results for the same compound (Polli et al. 2001). A variety of cell monolayer models that either mimic in vivo intestinal epithelium in humans such as Caco-2 cells or polarized cell lines stably transfected with MDR1 such as MDCKII-MDR1 have been developed and currently enjoy widespread popularity. Cell cultivation to obtain a tight, functional cell monolayer generally requires 1 to 3 weeks with three to nine laborious cell-feeding steps. Furthermore, these models require the determination of compound translocation from one compartment to another by means of HPLC-based methods that are compatible with high-throughput requirements only at high cost (Balimane and Chong 2005). Although regarded as state of the art, data obtained from such experiments can suffer bias from endogenous transporters expressed in the host cell line (Acharya et al. 2006; Goh et al. 2002) or nonselectivity of the inhibitors used (Evers et al. 2000). Furthermore, published data on ABCB1 function obtained from experiments using inside-out membrane vesicles obtained from ABCB1 overexpressing cells is scarce. The high passive permeability of ABCB1 substrates resulting in a low signal to noise ratio because of the rapid redistribution of the compounds has been reported as the principal experimental drawback in carrying out these experiments.

Given the reasons above, it is an important challenge to develop high-throughput, cost-effective, and highly predictive screening models to unambiguously categorize ABCB1 substrates, inhibitors, and inducers. The aim of this study was, therefore, to define such a rigorous, low-cost screening procedure amenable to high throughput for the identification of ABCB1 substrates and inhibitors that can be used in the early stages of drug discovery. We experimentally dissected the processes governing the translocation of small molecules across biological membranes and studied passive permeability and ABCB1-ATPase activity, a surrogate for ABCB1 function, independently. We determined passive permeability in an artificial membrane permeability assay (HDM-PAMPA) and compared the results with permeability values obtained in a tight paracellular system, i.e., MDCKII cell monolayer for a training set containing 40 INN drugs. Furthermore, using the same compound set, we compared vanadate-sensitive ABCB1-ATPase activity with data from cellular assays, i.e., Caco-2 monolayer efflux, and the calcein assay, commonly used to identify ABCB1 substrates and inhibitors, respectively. We subsequently tested the hypothesis that vanadate-sensitive ABCB1-ATPase activity can be successfully applied to identify ABCB1 substrates and inhibitors when combined with data on passive permeability in a validation set consisting of 26 development compounds.

Materials and methods

Chemicals

All generic drugs were purchased from Sigma-Aldrich (Schnelldorf, Germany). Ritonavir and fluvastatin were obtained from Toronto Research Chemicals (North York, ON, Canada), topotecan and doxorubicin were purchased from Alexis (Grünberg, Germany). Pantoprazole, pumafentrine, and tolafentrine were from Altana Pharma. GF120918 (GW918) was synthesized at Altana Pharma. KO143 was a kind gift of Dr. Gerrit-Jan Koomen, University of Amsterdam (Amsterdam, The Netherlands). [^{3}H]cimetidine and [^{3}H]methotrexate were acquired from Amersham Biosciences (Freiburg, Germany). [^{14}C]caffeine and [^{14}C]erythromycin were purchased from Perkin Elmer/NEN (Boston, MA, USA). [^{3}H]D-Mannitol was obtained from MP Biomedicals (Cambridge, UK), and [^{3}H]mitoxantrone from Biotrend (Cologne, Germany). Dulbecco's modified Eagle's medium and fetal calf serum, nonessential amino acids, and antibiotics were obtained from Biochrom (Berlin, Germany).

Training set

A set of 40 INN drugs was selected based on the compound's passive permeability (Wohnsland and Faller 2001) and their interaction with ABCB1. Compounds known to interact with ABCB1, i.e., cyclosporine A, digoxin, doxorubicin, erythromycin, lansoprazole, omeprazole, pantoprazole, prazosine, propranolol, pumafentrine, quinidine, ritonavir, and verapamil, were included in the compound set.

Validation set

Out of 1,296 small molecules originating from different chemical series for which ABCB1-ATPase and passive permeability using HDM-PAMPA had been determined at Altana Pharma, two subsets of compounds were selected. Subsets 1 and 2 contained compounds with molecular weights greater than 300 Da (to exclude paracellular transport) and mass balance between 0.8 and 1.2. All compounds stimulated basal ABCB1-ATPase activity. The compounds were discriminated according to their passive permeability with high permeable compounds (HDM-PAMPA P_{app} >50 cm×10^{-6} cm/s) grouped in subset 1 and low permeable compounds (HDM-PAMPA P_{app} <5 cm×10^{-6} cm/s) in subset 2.

Passive permeability

Artificial membrane permeability assay

Passive permeability was determined using hexadecane artificial membrane permeability assay (HDM-PAMPA) as described by (Wohnsland and Faller 2001) with hexadecane (700 nl/well) as artificial membrane. Assay plates were stirred on an orbital shaker (Teleshake, H&P Labortechnik, Oberschleißheim, Germany) at 100 rpm. Passive permeability was recorded after 5 or 96 h for compounds depending on high or low flux through the hexadecane layer. The sandwich was disassembled and the solutions in the acceptor and donor compartments were transferred to disposable UV-transparent plates (UV-Star®, Greiner-Bio-One, Frickenhausen, Germany). UV absorption was measured with a SAFIRE microplate spectrophotometer (Tecan, Männedorf, Switzerland) scanning each compound from 240 to 450 nm, recording each compound at individual wavelengths yielding maximal UV absorption. Mass balance conditions were verified in order to assess retention of test compounds to the hexadecane layer or unspecific binding to assay plates.

MDCKII permeability assay

Madin–Darby canine kidney (MDCKII) cells (Evers et al. 1998) were obtained from The National Cancer Institute (Amsterdam, The Netherlands). The cells were grown in culture medium consisting of Dulbecco's modified Eagle's medium (DMEM) with L-GlutaMax® (4.5 g/L glucose; Invitrogen, The Netherlands), supplemented with heat-inactivated fetal calf serum (10% *v*/*v*), 100 U/mL penicillin, and 100 μg/mL streptomycin.

Cells from passage 6 to passage 25 were used for transport experiments. Cells were seeded and cultured as reported earlier (Evers et al. 1998). Culture medium was removed from the filter inserts and washed with HBSS and placed to a new 12-well plate (Costar, Cambridge, MA, USA) that had been pretreated by 24 h incubation with culture medium. The transport was started by the addition of 650 μL of 10 or 100 μM compound dissolved in HBSS to the apical compartment. A 150 μL sample was taken afterwards from the donor compartment at t=0 min to determine the initial concentration of substrate (C_0) and stored at <−18°C until further analysis. The plates, containing the filter inserts, were subsequently incubated in a humidified incubator at 37°C for 120 min being stirred on an orbital shaker at 100 rpm. Samples from the basolateral compartment (400 μL) were collected and stored at <−18°C. Markers for paracellular and transcellular flux, i.e., [^{3}H]mannitol and [^{14}C]caffeine, were assayed in parallel in each set of experiments. Mass balance conditions were verified by additional sampling in the donor compartment in order to assess retention of test compounds to the cell monolayer or unspecific binding to assay plates.

ABCB1-ATPase

Stimulation of basal ABCB1-ATPase activity

Stimulation of basal ABCB1-ATPase activity was measured as described earlier (Sarkadi et al. 1992). ABCB1 containing membrane fraction were obtained from Solvo Biotechnology (Budaörs, Hungary). Membrane vesicles (15 μg/well) were incubated in 5 mM $MgCl_2$, 50 mM MES–Tris (pH 7.0), 50 mM KCl, 2 mM dithiothreitol, 0.1 mM ethylene glycol bis(2-aminoethyl ether)-*N*,*N*,*N*′,*N*′-tetraacetic acid, 5 mM sodium azide, 1 mM ouabain, 5 mM ATP, and with at least eight different concentrations of test compounds dissolved in DMSO with and without the presence of 0.4 mM sodium orthovanadate for 50 min at 35°C. The maximal amount of DSMO added to the assay medium was 2%. ABCB1-ATPase activities were determined as the difference of inorganic phosphate liberation measured with and without the presence of 400 μM sodium orthovanadate (vanadate-sensitive ATPase activity). The amount of inorganic phosphate released was determined as described earlier (Sarkadi et al. 1992) or using the PREDEASY™ kit (Solvo Biotechnology, Budaörs, Hungary). DMSO and 40 μM verapamil were used as

negative and positive controls for ABCB1-ATPase activation, respectively. ATPase assays were carried out in 96-well plates (Nunc, Wiesbaden, Germany), either by hand or automatically with a Tecan EVO robot (Tecan, Männedorf, Switzerland). All incubations were carried out in duplicate.

Inhibition of stimulated ABCB1-ATPase activity

Inhibition of stimulated ABCB1-ATPase activity was essentially determined as described above upon stimulation with 40 μM verapamil. ABCB1-ATPase activities in the presence of at least two different concentrations of test compounds relative to verapamil-stimulated control were determined. All incubations were carried out in duplicate.

ABCB1 inhibition: calcein assay

K562-MDR cells overexpressing ABCB1 were obtained from Dr. Sarkadi (National Medical Centre, Institute of Haematology and Immunology, Budapest, Hungary). The cells were cultured as previously described (Homolya et al. 1996). After centrifugation at 500×*g*, culture medium was removed and cells were resuspended in HBSS, pH 7.4, at 1×10^6 cells/mL. One hundred microliters of this suspension was added to each well of a 96-well plate (Corning, Corning NY, USA). Test drugs (seven 1:3 serial dilutions ranging from 100 to 0.08 μM final concentration) and controls dissolved in DMSO were added at a volume of 2 μL and preincubated for 15 min at 37°C. Calcein acetoxymethylester (calcein AM) dissolved in HBSS containing 50 μg/mL bovine serum albumin (BSA) was added to a final concentration of 250 nM, i.e., K_m value of calcein AM efflux in K-562-MDR cells (Essodaigui et al. 1998), to each well and fluorescence (excitation 485 nm, emission 538 nm) was recorded every 30 s for 8 min to ensure initial permeability rate conditions. The rate at which fluorescent calcein was detected reflects the measurement of ABCB1 inhibition. Notably, the fluorescence increases with increasing inhibition of ABCB1-mediated efflux of calcein AM. The permeability rate of calcein AM was determined by calculating the slope of the fluorescence recorded over 8 min plotted relative to the fluorescence in the presence of 60 μM verapamil (positive control, 100%) and DMSO (blank control, 0%). We used propidium iodine staining as a control to detect possible disruption of cell membrane integrity caused by the test compounds. Altana Pharma licensed the use of the calcein assay from Solvo Biotechnology.

ABCB1 function: Caco-2 assay

Caco-2 cells (batch no. 2463691) were obtained from the American Type Culture Collection (ATCC, Manassas, VA, USA) at passage 17. The cells were grown in culture medium consisting of DMEM (Biochrom, Berlin, Germany), supplemented with glutamine, 4.5 g/L glucose, heat-inactivated fetal calf serum (20% *v*/*v*), 100 U/mL penicillin, and 100 μg/mL streptomycin as described earlier (Yee 1997).

For transport studies, cells from passage 55 to 70 were used by seeding them on semipermeable filter inserts (24 wells inserts, 0.4 μm pore size; Greiner-BioOne, Frickenhausen, Germany) at 2×10^5 cells/cm^2. The cells on the inserts were then cultured for 21 to 25 days prior to use. For transport experiments new 24-well plate (Greiner-BioOne, Frickenhausen, Germany) that had been pretreated by incubating 24 h with culture medium were used. The transport buffer was HBSS buffer containing 20 mM HEPES and 20 mM glucose monohydrate. The pH of both the apical and basolateral compartments was 7.4. The transport was started by the addition of 350 μL of 10 or 100 μM compound dissolved in transport buffer to the apical compartment. Subsequently, a 50 μL sample was taken from the donor compartment at $t=0$ min to determine the initial concentration of substrate (C_0) and stored at <−18°C until further analysis. Then, 750 μL transport buffer was added to the 24-well plates, i.e., the basolateral compartment. The plates, containing the filter inserts, were then incubated in a humidified incubator at 37°C for 120 min being stirred on an orbital shaker at 300 rpm. Samples from both compartments were collected and stored at <−18°C. Markers for paracellular and transcellular flux, i.e., FITC-dextran and propranolol, were assayed in parallel in each set of experiments.

ABCB1 function, i.e., the effect of ABCB1 on the permeability of test compounds in the absorptive (apical to basolateral) direction, was assessed by calculating the ratio of apparent permeability coefficients in the presence and absence of the ABCB1 inhibitor GF120198 or the ABCG2 inhibitor KO143, added to the apical and basolateral compartment at 1 μM. The ratio of digoxin permeabilities was determined for each batch of Caco-2 monolayer in the presence and absence of 1 μM GF120198 to ensure comparable ABCB1 expression. Only Caco-2 monolayer exhibiting digoxin permeability ratios >2.5 were used for further experiments. Mass balance conditions were verified by additional sampling in the donor compartment in order to assess retention of test compounds to the cell monolayer or unspecific binding to assay plates. All experiments were carried out in triplicate.

Sample analysis

All compounds were determined using an Agilent HPLC System 1100 (Agilent, Waldbronn, Germany) equipped with a binary pump. Compounds in set 1 were eluted using a

Synergy Fusion 4.0 μm particle size, 75×4.6 mm reversed phase column (Phenomenex, Darmstadt, Germany) in combination with a RP18 security guard 10×3.0 mm precolumn as stationary phase. The mobile phases were: (A) 10 mM ammonium acetate buffer, pH 3.0 or 6.0 and (B) acetonitrile. Compounds in set 2 were eluted using a Synergy Fusion, Mercury MS 2.0 μm particle size, 20×4.0 mm reversed phase column (Phenomenex, Darmstadt, Germany) as stationary phase. The mobile phases were: (A) 10 mM potassium dihydrogen phosphate, pH 3.0 or 10 mM ammonium acetate buffer pH 6.0 and (B) acetonitrile.

[^{14}C]- and [^{3}H]-labeled compounds were determined by liquid scintillation counting on a Wallac Pharmacia S1414 scintillation counter (Perkin Elmer, Rodgau, Germany); all samples were counted for 10 min or at least 10,000 counts.

Western blot analysis

Caco-2 monolayer were grown on six-well plates as described for transport experiments. Isolation of human enterocytes and the preparation of cell homogenates were carried out as described earlier (von Richter et al. 2004), except for the use of Complete® Mini Protease Inhibitor Cocktail Tablets (Roche Diagnostics, Manheim, Germany) as protease inhibitors. The detection of ABCB1 was performed using the anti-ABCB1 monoclonal antibody F4 (Sigma Immunochemicals, Deisenhofen, Germany) as reported earlier (Greiner et al. 1999). Western blotting of ABCG2 was carried out loading 50 μg cell homogenate. The blots were blocked for 1 h at room temperature with 5% (wt/vol) BSA in TBS-T (0.1% [vol/vol] Tween 20, 15 mM sodium chloride, and 1 mM Tris hydrochloride; pH 7.4). The blots were then incubated for 1 h at room temperature with the anti-MXR monoclonal antibody BXP-21 (Alexis Biochemicals, Grünberg, Germany) diluted 1:50 in TBS-T containing 5% (wt/vol) BSA and subsequently washed four times with TBS-T and following incubation with a mixture of antimouse peroxidase labeled and a streptavidin conjugate diluted 1:50,000 in TBS-T for 2 h at room temperature. After washing the blots four times with TBS-T, all proteins were detected by means of chemiluminescence (Lumi-light Roche Diagnostics, Mannheim Germany) and a charged-coupled device camera (Fuji LAS-1000; Raytest, Straubenhardt, Germany). Signal intensities were measured by use of the AIDA 2.31 software (Raytest).

Data analysis

Apparent permeability

The apparent permeability coefficients (P_{app}) for experiments carried out under non-sink conditions using HDM-PAMPA, MDCKII-cells, and Caco-2 cells were calculated according to Wohnsland and Faller (2001) as follows:

$$P_{app} = -1\frac{V_D \times V_R}{(V_D + V_R) \times A \times \varepsilon_a \times t} \times \ln\left(1 - \frac{C_R(t)}{C_{Eq}}\right) \quad (1)$$

where V_D is the volume of the donor compartment, V_R is the volume of the acceptor compartment, A is the accessible filter area, t is the incubation time, $C_R(t)$ is the concentration in the receiver compartment at time point t, and C_{Eq} is the concentration corresponding to a full equilibrium of the compound in the donor and acceptor compartment. The P_{app} was corrected for the apparent porosity (ε_a) according to Nielsen and Avdeef (2004) using ε_a−HDM-PAMPA= 0.495 and ε_a−MDCKII, Caco-2=1.0.

A retention factor (R_M) for all permeability experiments was calculated to assess mass balance conditions as follows:

$$R_M = 1 - \frac{C_D(t) + C_R(t)}{C_0} \quad (2)$$

where $C_D(t)$ and $C_R(t)$ are the concentrations in the donor and receiver compartment, respectively, at time point t.

ABCB1-ATPase kinetics

V_{max} and K_m values for the formation of inorganic phosphate from ABCB1-ATPase experiments were estimated by analysis of untransformed reaction velocity data via nonlinear regression. Compounds that stimulated ABCB1-ATPase activity without inhibition (ATPase type A) were fitted to a modified form of the Michaelis–Menten equation:

$$V_S = V_0\frac{(V_{max} - V_0)S}{(S + K_m)} \quad (3)$$

where V_S is the ATPase activity as a function of the substrate concentration S and V_0 is the basal activity (the activity in the absence of modulator).

Drugs that stimulated ATPase activity at low concentrations but inhibit activity at higher concentrations (ATPase type B) were fitted using Eq. 2:

$$V_S = \frac{K_1K_2V_0 + K_2V_1S + V_2S^2}{K_1K_2 + K_2S + S^2} \quad (4)$$

where V_S is the ATPase activity as a function of the substrate concentration S and V_0 is the basal activity (the activity in the absence of modulator). V_1 is the maximal enzyme activity if only activation occurred and K_1 is the substrate concentration that gives the half-maximal increment in this ATPase activity. V_2 is the activity at infinite concentration of the modulator and K_2 is the substrate concentration that gives half-maximal reduction of ATPase

activity from the value V_1. This equation is based on conventional enzyme kinetics algebra for a model that has an activity V_1 with one substrate molecule (S) bound and a lower activity 1 of magnitude V_2 with two substrates (S) molecules bound (Litman et al. 1997a). The data were analyzed by use of the GraphPad Prism software (version 4.0; GraphPad, San Diego, USA).

ABCB1-ATPase assay robustness

In order to assess the robustness of the ABCB1-ATPase assay, assay variability and signal dynamic range were combined according to Zhang et al. (1999), calculating Z' factors. Positive controls (DMSO) and negative controls (40 μM verapamil) containing 0.4 mM vanadate to determine Z' factors for vanadate-sensitive ABCB1-ATPase activity were used. Z' factors were determined for the ABCB1 assay in a 96-well format carried out manually using the PREDEASY™ kit and automated on a Tecan EVO robot (Tecan, Männedorf, Switzerland) using a phosphate detection method described by Sarkadi et al. (1992).

ABCB1 inhibition

The inhibitory potency of compounds subjected to the calcein assay was expressed as IC_{50} (concentration leading to half-maximal inhibition). The IC_{50} values were calculated using the four-parameter equation with a variable slope:

$$\text{Inhibition} = \frac{\text{Bottom} + (\text{Top} - \text{Bottom})}{1 + 10^{((\log IC_{50} - S) \times h)}} \quad (5)$$

where Bottom is the minimal inhibition observed, Top is the maximal inhibition observed, and h refers to the Hill constant.

Statistical analysis

The distribution of permeability data was analyzed by the method of Kolmogorov and Smirnov using the GraphPad Prism software (Version 4.0; GraphPad, San Diego, CA, USA). Correlation analyses were performed by the use of the Pearson product moment correlation with a value of $P<0.05$ regarded as statistically significant because not all data passed the normality test.

Results

Passive permeability: comparison of HDM-PAMPA with MDCKII cell monolayer

Passive apparent permeability coefficients ($P_{app\text{-}HDM}$) in training set determined with HDM-PAMPA ranged from 0.02 cm×10^{-6}/s to 210 cm×10^{-6}/s (Table 1). P_{app} determined through MDCKII cell monolayer in the apical to basolateral direction ranged from 0.89 cm×10^{-6}/s to 199 cm×10^{-6}/s and from 0.73 cm×10^{-6}/s to 165 cm×10^{-6}/s in the presence of 1 μM GF120918 for the same set of compounds. The logarithmic transformed data obtained from HDM-PAMPA exhibited a good correlation with P_{app} determined in MDCKII cell monolayer for the training set compounds (r_s=0.84, cp. Fig. 1). A similar correlation was found when $P_{app\text{-}HDM}$ were correlated with data obtained from MDCKII cell monolayer in the presence of 1 μM GF120918 (r_s=0.87, cp. Fig. 1).

ABCB1-ATPase training set

The effects of compounds contained in the training set that interacted with ABCB1-ATPase activity fall into three main categories listed in Table 1: compounds that stimulate basal ABCB1-ATPase activity (ABCB1-ATPase type A), drugs that stimulate basal ABCB1-ATPase activity at low concentrations but inhibit the activity at higher concentrations (ABCB1-ATPase type B), and compounds that inhibit basal and/or verapamil-stimulated ABCB1-ATPase activity (ABCB1-ATPase type C). Examples of concentration–response curves are given in Fig. 2. None of the compounds that interacted with ABCB1-ATPase changed ATPase activity of membrane fractions prepared from empty control vector-infected cells (data not shown). ATPase background activity in the training set, i.e., the vanadate-sensitive ATPase activity measured in the DMSO controls in membrane fractions containing ABCB1, was on average 5.86±1.07 nmol P_i/mg/min (range 4.00–8.60 nmol P_i/mg/min) which is close to the ATPase activity in cholesterol-depleted MDR1-transfected Sf9 membrane vesicles reported earlier (Garrigues et al. 2002a). Mean ATPase background activity determined in membrane fractions prepared from empty control vector-infected cells was 4.16±0.47 nmol P_i/mg/min (range 3.74–4.91 nmol P_i/mg/min) and ranged close to the LLOQ of the phosphate detection method used for the automated ATPase assay (3.12 nmol P_i/mL corresponding to an ATPase activity of 3.47 nmol P_i/mg/min). ABCB1-ATPase stimulation with 40 μM verapamil amounted to 25.6 nmol P_i/mg/min, yielding a signal to background ratio of 4.6 that was in the same range as reported by others (Ambudkar et al. 1992; Sarkadi et al. 1992). The apparent K_m of the stimulation of ABCB1-ATPase activity was obtained at 0.5 mM ATP. No correlation was found between the apparent K_m value of the training set compounds stimulating ABCB1-ATPase and passive permeability determined with HDM-PAMPA (r_s=−0.06, P=0.43, N=11). Given the small variability of both vanadate-sensitive ABCB1-ATPase background activity and verapamil-stimulated

Table 1 ABCB1-ATPase activity, calcein AM, HDAM-PAMPA, and Caco-2 data for training set (N=40 INN compounds)

No.	Compound	ATPase V_0/V_{max} (nmol/mg/min)	ATPase K_1 (μM)	ATPase type	Calcein IC_{50} (μM)	Calcein Hill factor	P_{app} HDM-PAMPA ($cm \times 10^{-6}/s$]	MDCKII P_{app} a–b ($cm \times 10^{-6}/s$)	Caco-2 P_{app} a–b ($cm \times 10^{6}/s$)	Caco-2 P_{app} a–b_{GF} ($cm \times 10^{6}/s$)	Caco-2 GF120918 ratio[a]
1	Acyclovir	–/–	–	Nonsubstr.	No inhib.	–	0.05	2.23	2.00	2.00	1.00
2	Alprenolol	5.6/18.6	163	A	181	1.01	94.7	51.3	144	153	1.06
3	Amiloride	–/–	–	Nonsubstr.	No inhib.	–	0.03	2.54	4.79	3.73	0.78
4	Antipyrine	–/–	–	Nonsubstr.	No inhib.	–	8.81	84.7	196	150	0.77
5	Atenolol	–/–	–	Nonsubstr.	No inhib.	–	0.47	1.31	1.91	1.88	0.98
6	Ceftriaxon	–/–	–	Nonsubstr.	No inhib.	–	0.15	2.09	2.46	2.75	1.12
7	Chloramphenicol	–/–	–	Nonsubstr.	No inhib.	–	1.02	17.5	46.4	51.6	1.11
8	Chloroquine	–/–	–	Nonsubstr.	No inhib.	–	25.7	24.0	9.06	8.68	0.96
9	Cimetidine	–/–	–	Nonsubstr.	No inhib.	–	0.20	2.31	0.93	0.99	1.06
10	Cyclosporine A	9.6/8.9	0.138[b]	C	0.247	1.58	28.2	3.93	7.66	6.26	0.82
11	Desipramine	6.9/38.2	>250	A	221	1.55	210	38.3	80.3	82.8	1.03
12	Digoxin	6.8/17.3	83.7	A	189	1.41	0.62	3.20	4.44	12.1	2.73
13	Doxorubicin	4.2/29.1	>250	A	n.a.[c]	n.a.[c]	0.05	1.05	1.44	2.40	1.67
14	Erythromycin	6.7/17.6	45.0	A	130	3.52	5.05	n.a.	1.70	2.92	1.72
15	Fluvastatin	7.5/8.0	38.3[b]	C	151	0.70	0.16	30.7	22.8	31.0	1.36
16	Furosemide	–/–	–	Nonsubstr.	No inhib.	–	0.06	2.11	1.94	1.94	1.00
17	Guanabenz	4.0/96.8	>250	A	>250	0.93	5.77	113	165	158	0.96
18	Imipramine	6.1/66.3	78.4	A	180	0.64	129	154	99.0	121	1.22
19	Lansoprazole	5.3/30.0	57.0	A	86.9	0.81	23.0	69.0	150	150	1.00
20	Levodopa	–/–	–	Nonsubstr.	No inhib.	–	n.a.[d]	n.a.[d]	n.a.[d]	n.a.[d]	n.a.[d]
21	Methotrexate	–/–	–	Nonsubstr.	No inhib.	–	0.02	0.91	7.37	6.72	0.91
22	Metoprolol	–/–	–	Nonsubstr.	No inhib.	–	7.88	90.0	145	131	0.90
23	Midazolam	7.0/20.0	22.5	A	73.9	0.72	106	54.1	213	210	0.99
24	Mitoxantrone	–/–	–	Nonsubstr.	No inhib.	–	0.03	3.06	0.12	0.18	1.50
25	Naproxen	–/–	–	Nonsubstr.	No inhib.	–	3.60	65.4	109	103	0.95
26	Omeprazole	5.7/42.9	118	A	80.5	1.49	14.3	59.0	144	135	0.94
27	Pantoprazole	5.4/31.5	>250	A	108	1.18	5.25	49.5	121	146	1.21
28	Prazosine	5.6/47.0	55.0	A	28.7	1.41	3.13	25.6	14.1	16.6	1.18
29	Propranolol	6.3/15.4	>250	A	>250	0.39	78.1	82.3	147	135	0.92
30	Pumafentrine	7.3/7.4	6.97[b]	C	3.12	1.68	79.0	40.3	71.9	82.0	1.14
31	Quinidine	6.3/18.3	8.3	A	4.39	0.65	26.6	43.2	112	108	0.96
32	Ranitidine	–/–	–	Nonsubstr.	No inhib.	–	0.04	1.42	3.99	4.90	1.23
33	Ritonavir	5.0/32.8	0.28/9.13	B	2.86	1.77	3.50	32.0	81.1	108	1.33
34	Sulfasalazine	–/–	–	Nonsubstr.	No inhib.	–	0.03	1.79	0.87	0.82	0.94
35	Sulpiride	–/–	–	Nonsubstr.	No inhib.	–	0.04	0.89	2.70	2.81	1.04
36	Terbutaline	–/–	–	Nonsubstr.	No inhib.	–	0.26	2.59	1.47	1.72	1.17
37	Testosterone	5.0/32.5	>250	A	56.4	1.68	71.2	199	n.a.[d]	n.a.[d]	n.a.[d]
38	Tolafentrine	5.5/11.2	5.29	A	9.46	1.71	3.31	10.4	20.3	29.2	1.44
39	Topotecan	7.3/7.4	81.2[b]	C	n.a.[c]	n.a.[c]	0.61	2.30	2.63	7.15	2.72
40	Verapamil	5.6/25.9	4.78	A	2.61	0.97	98.2	55.2	113	159	1.41

ABCB1-ATPase activity was categorized as follows: compounds that stimulate basal ABCB1-ATPase activity (type A), drugs that stimulate basal ABCB1-ATPase activity at low concentrations but inhibit the activity at higher concentrations (type B), and compounds that inhibit basal and/or verapamil-stimulated ABCB1-ATPase activity (type C) or compounds that do not interact with ABCB1-ATPase activity (nonsubstr.) or compounds that did not inhibit calcein AM efflux from K562-MDR cells over the concentration range tested (No inhib.)

[a] ABCB1 function, i.e., the effect of ABCB1 on the permeability of test compounds in the absorptive (apical to basolateral) direction expressed as the ratio of apparent permeability coefficients in the presence and absence of 1 μM GF120198

[b] IC_{50} value for the inhibition of verapamil-stimulated ABCB1-ATPase

[c] For doxorubicin and topotecan no data could be provided due to damage of the cells reflected by propidium iodine staining

[d] For testosterone and levodopa no data could be obtained in Caco-2 and/or MDCKII cell monolayers due to extensive metabolism of the compounds

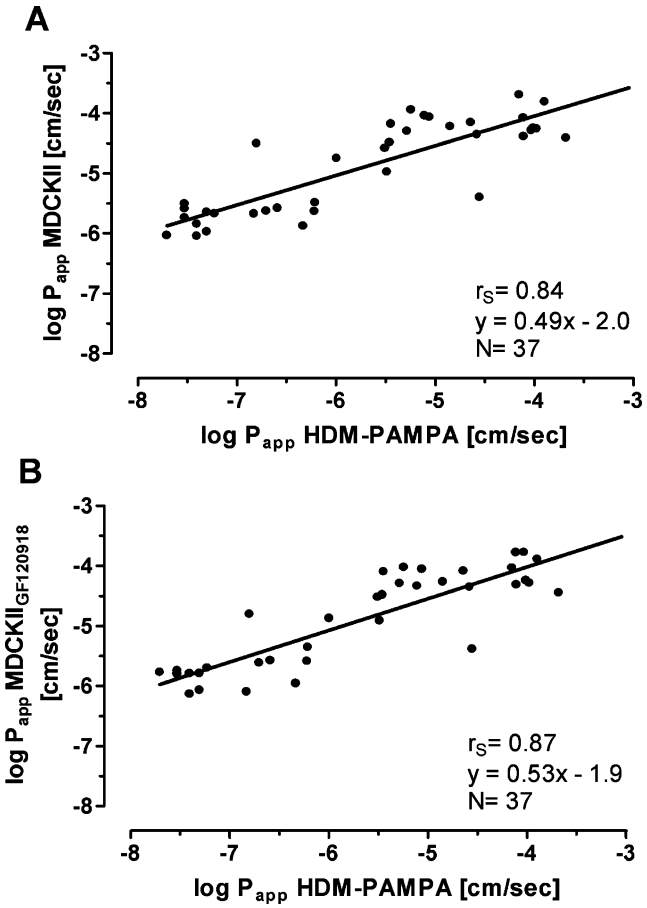

Fig. 1 Correlation analysis of apparent passive permeability (P_{app}) obtained for 37 training set compounds. Logarithmic transformed apparent permeability (P_{app}) obtained from HDM-PAMPA was correlated with P_{app} determined trough MDCKII cell monolayers under control conditions (**a**) or in the presence of 1 μM GF120918 (**b**). The *solid line* represents the linear regression line

activity, the robustness of the assay reflected by *Z'* factors generated manually with the PREDEASY™ kit (0.80) or with the automated assay (0.54) was excellent.

ABCB1 inhibition: training set

Out of the 40 compounds contained in the training set, 20 inhibited ABCB1-mediated efflux of calcein AM out of K562-MDR cells. The IC_{50} values ranged from 0.247 μM (cyclosporine A) to 221 μM (desimipramine). The Hill constant obtained for the 20 compounds inhibiting ABCB1-mediated efflux of calcein AM was 1.29±0.68. Doxorubicin and topotecan increased the permeability of propidium iodine in control experiments suggesting possible disturbances of K562-MDR cell integrity and were, therefore, omitted from the analysis. With the exception of digoxin and fluvastatin, passive permeability obtained with HDM-PAMPA was >3.0 cm×10^{-6}/s for all compounds that inhibited ABCB1-mediated efflux of calcein AM out of K562-MDR cells (Fig. 3a).

All compounds that stimulated basal ABCB1-ATPase activity inhibited calcein efflux except for cyclosporine A, fluvastatin, and pumafentrine. These compounds were subsequently analyzed whether they alter basal ABCB1-ATPase activity depending on ATP concentration or whether they could inhibit verapamil-stimulated ABCB1-ATPase activity. Neither of the compounds stimulated basal ABCB1-ATPase analyzed with ATP concentrations ranging from 0.5 to 5.0 mM (data not shown). However, cyclosporine A, fluvastatin, and pumafentrine inhibited verapamil-stimulated ABCB1-ATPase activity with IC_{50} values of 0.138, 38.3, and 6.97 μM, respectively, and were, therefore, classified as type C compounds. All compounds stimulating basal ABCB1-ATPase activity (type A/B) contained in the training set were not found to inhibit verapamil-stimulated ABCB1-ATPase activity (data not shown).

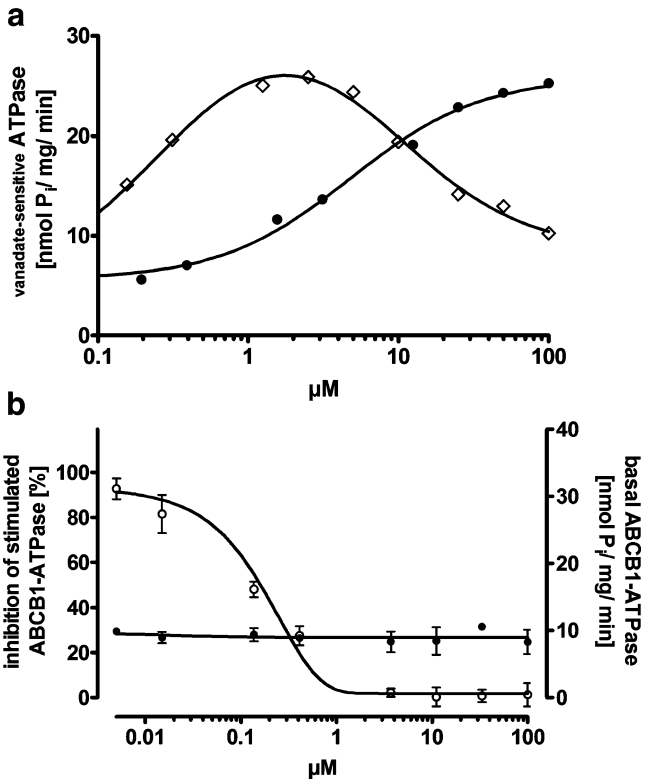

Fig. 2 **a** Examples of differences in vanadate-sensitive ABCB1-ATPase activity stimulating drugs; verapamil (ABCB1-ATPase type A), compounds that stimulate basal ABCB1-ATPase activity; ritonavir (ABCB1-ATPase type B), drugs that stimulate basal ABCB1-ATPase activity at low concentrations but inhibit the activity at higher concentrations. **b** Examples of differences on basal vanadate-sensitive ABCB1-ATPase activity (right *x*-axis) and vanadate-sensitive, verapamil-stimulated ABCB1-ATPase activity (left *y*-axis) of cyclosporine (ABCB1-ATPase type C) as an example of compounds that inhibit basal and/or verapamil-stimulated ABCB1-ATPase activity

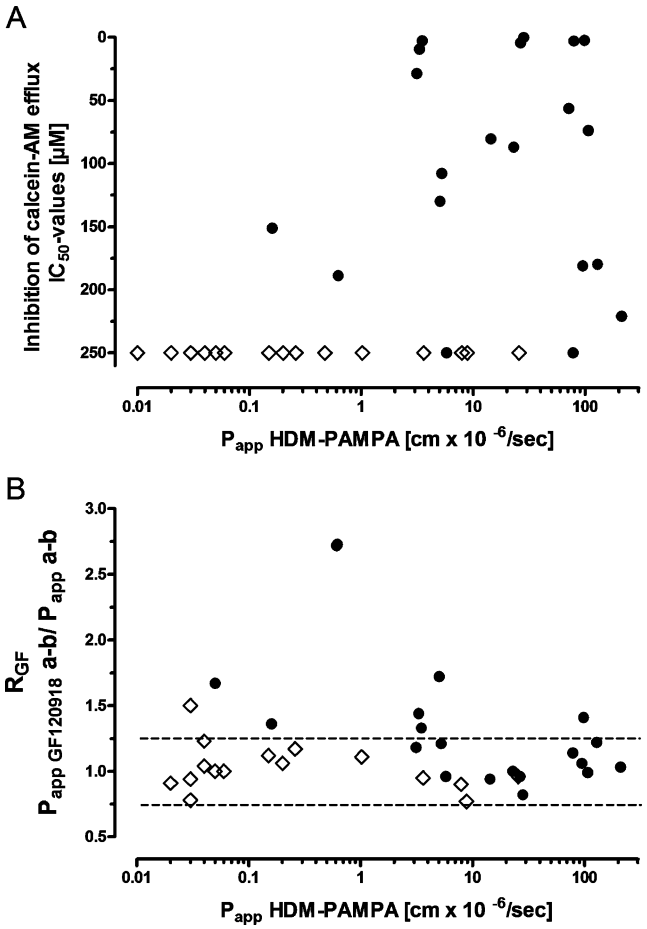

Fig. 3 **a** Correlation between the IC_{50} value for the inhibition of calcein AM efflux from K562-MDR1 cells and passive permeability determined with HDM-PAMPA of training set compounds interacting with ABCB1-ATPase (types A, B, C; *filled circles*) and ABCB1 nonsubstrates (*open diamonds*) contained in the training set. For better visualization, the IC_{50} value for ABCB1 nonsubstrates was arbitrarily set to 250 μM. **b** Correlation between ABCB1 function determined as the ratio of apparent permeability across Caco-2 cells in the presence and absence of 1 μM GF120198 and passive permeability determined with HDM-PAMPA of training set compounds. The *broken line* indicates the threshold ratios of 1.25 and 0.75 discriminating a compound that is actively transported. ABCB1 substrates (ATPase types A, B, C; *filled circles*) and ABCB1 nonsubstrates (*open circles*) were assessed using ABCB1-ATPase activity

ABCB1 function: training set

At first, we characterized the cellular system, i.e., Caco-2 cell monolayer, used to identify ABCB1 substrates. ABC transporter expression has been shown to be highly variable in Caco-2 cells depending on the cell batch used, cell culture media, filter membranes, and postseeding cultivation time. The amounts of ABCB1 and ABCG2 in the Caco-2 cell monolayer used were compared relative to the abundance of the two proteins in human enterocytes by means of Western blotting. As depicted in Fig. 4, the expression of ABCB1 in Caco-2 cells relative to human enterocytes was 129%. In addition, almost equal amounts (84%) of ABCG2 were found in the Caco-2 cells when compared with the relative amount expressed in human enterocytes.

ABCB1 function was assessed as the effect of ABCB1 on the flux of test compounds in the apical to basolateral, i.e., the absorptive, direction by calculating the ratio of compound flux in the presence and absence of the ABCB1 inhibitor GF120198. Based on a mean coefficient of variation of 11.6% over all Caco-2 experiments, i.e., the average experimental error, the threshold ratio discriminating compound transported by ABCB1 from a nontransported compound, was set at 1.25, assuming an additive error resulting from the two measurements. For digoxin, doxorubicin, erythromycin, fluvastatin, mitoxantrone, ritonavir, topotecan, tolafentrine, and verapamil, ratios of >1.25 were obtained, indicating a net effect of ABCB1 on compound flux in the apical to basolateral direction (Table 1). All of these compounds, except mitoxantrone, interacted with basal or verapamil-stimulated ABCB1-ATPase activity. However, ABCB1-ATPase activity alone did not predict the effect of ABCB1 on compound permeability in the apical to basolateral direction (Fig. 5a). With the exception of verapamil, all compounds for which a net effect of ABCB1 on compound flux in Caco-2 cell monolayer was observed, passive permeability obtained with HDM-PAMPA was <5.0 $cm \times 10^{-6}/s$ (Fig. 3b). In contrast, for none of the compounds, except for verapamil,

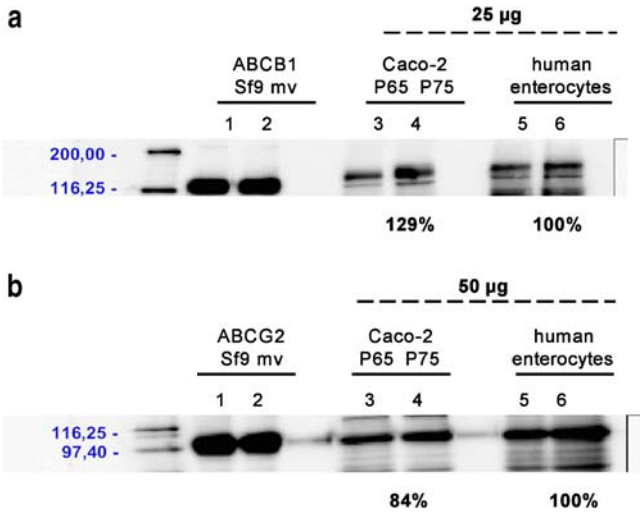

Fig. 4 ABCB1 (**a**) and ABCG2 (**b**) protein expression in Caco-2 cells relative to human enterocytes. ABCB1 or ABCG2 expressed in Sf9 membrane fractions (*lanes 1* and *2*, 5 mg in each lane), different amounts of Caco-2 cell homogenates from passage 65 (*lane 3*) or 75 (*lane 4*), and human enterocytes homogenate pooled from five donors (*lanes 5* and *6*) were subjected to Western blotting as described in the "Materials and methods" section. The percentages indicate the average amount of the ABCB1 and ABCG2 protein bands relative to the signal obtained in the human enterocyte sample

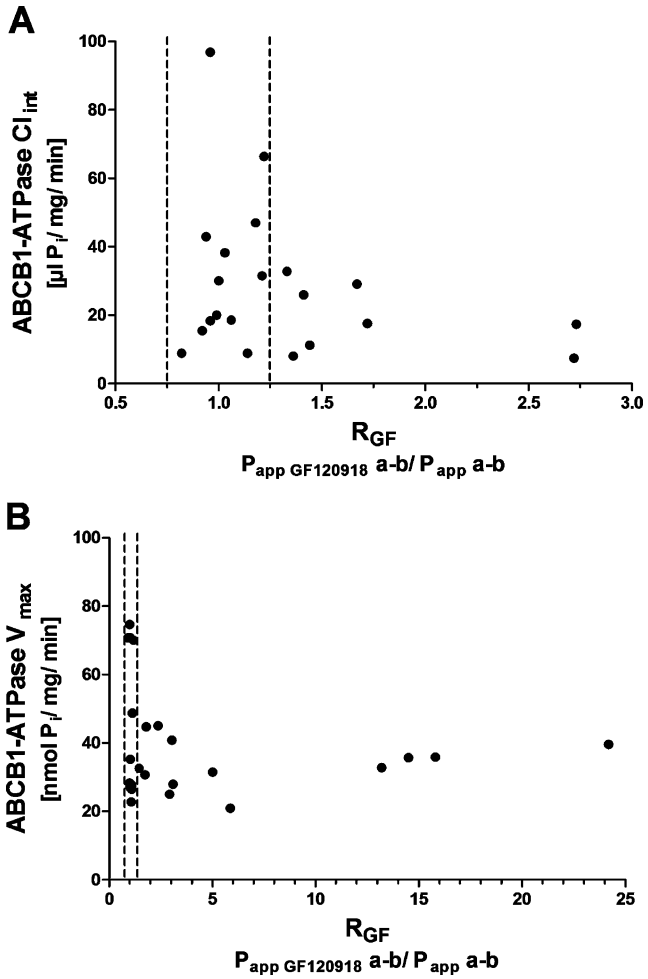

Fig. 5 Correlation of basal vanadate-sensitive ABCB1 ATPase activity (V_{max}) and ABCB1 function determined as the ratio of apparent permeability across Caco-2 cells in the presence and absence of 1 mM GF120198 for the training set (**a**) and validation set (**b**) compounds interacting with ABCB1 ATPase. The *broken line* indicates the threshold ratios of 1.25 and 0.75 discriminating a compound that is actively transported

that interacted with basal or drug-stimulated ABCB1-ATPase activity and inhibited calcein AM efflux, a net effect of ABCB1 on compound flux in Caco-2 cells was observed (Fig. 3a).

Mitoxantrone and topotecan have been found to be substrates of ABCG2 (*BCRP*) (Kruijtzer et al. 2002), and the Caco-2 monolayer contained ABCG2 that is also inhibited by GF120918 (Kruijtzer et al. 2002). Therefore, the effect of the ABCG2-specific inhibitor KO143 (Allen et al. 2002) on flux of both compounds in the apical to basolateral direction was additionally analyzed in order to assess the contribution of ABCG2 to the overall effect of GF120918. The ABCB1 probe drug digoxin was included in this analysis. GF120918 increased digoxin flux by 2.5-fold whereas KO143 had no effect. GF120918 and KO143 increased topotecan flux by 2.6-fold and 1.6-fold, respectively, whereas mitoxantrone flux was modestly increased by both inhibitors to the same extent (1.4-fold).

Passive permeability/ABCB1-ATPase: validation set

In order to verify whether passive permeability is an important covariate for compounds interacting with ABCB1-ATPase activity, we analyzed an additional compound set (N=26) that was selected out of 1,296 small molecules originating from different chemical series at Altana Pharma. Only compounds that stimulated ABCB1-ATPase activity were selected and stratified based on passive permeability that had been determined using HDM-PAMPA. The mean $P_{app\text{-}HDM}$ for compounds grouped in subset 1 (Table 2, compounds BYK1 to BYK13) was high (±82.1 cm×10^{-6}/s, range ±32.5–202 cm×10^{-6}/s) whereas subset 2 (Table 2, compounds BYK14 to BYK26) contained low $P_{app\text{-}HDM}$ compounds (mean ±0.29 cm×10^{-6}/s, range ±0.03–1.00 cm×10^{-6}/s). The K_m values for the stimulation of ABCB1-ATPase activity were comparable in both subsets (Fig. 6a) with a mean K_m value of 24.9 µM (range 2.07–100 µM) in subset 1 and 18.5 µM (range 1.89–45.2 µM) in subset 2.

ABCB1 inhibition: validation set

Although the K_m values for the stimulation of ABCB1-ATPase activity were comparable in both subsets (Fig. 6a), the IC_{50} values obtained with a cellular ABCB1 inhibition carried out under initial permeability rate conditions were not. The mean IC_{50} values for the inhibition of ABCB1-mediated efflux of calcein AM out of K562-MDR cells were 21.8 µM (range 3.61–95.3 µM) in subset 1 and 113 µM (range 17.0–256 µM) in subset 2 (cp. Fig. 6b). Two compounds in subset 2, i.e., BYK021 and BYK026, did not inhibit calcein AM efflux over the concentration range tested (Table 2). The Hill constants were comparable in both subsets (subset 1: mean 1.38, range 0.79–2.24; subset 2: mean 1.36, range 0.67–2.20). The comparison of K_m values for the stimulation of ABCB1-ATPase with IC_{50} values obtained with a cellular ABCB1 inhibition assuming a competitive inhibition revealed further differences. The ratio of calcein AM IC_{50} over ATPase K_m in subset 1 with a mean of 1.43 (range 0.27–2.60) was markedly different from subset 2 (mean 9.13, range 1.32–21.2). The individual comparisons of ABCB1-ATPase K_m values with IC_{50} values obtained for cellular ABCB1 inhibition are plotted in Fig. 6c and d.

ABCB1 function: validation set

For all low $P_{app\text{-}HDM}$ compounds contained in subset 2, an effect of ABCB1 on compound flux in Caco-2 cells was

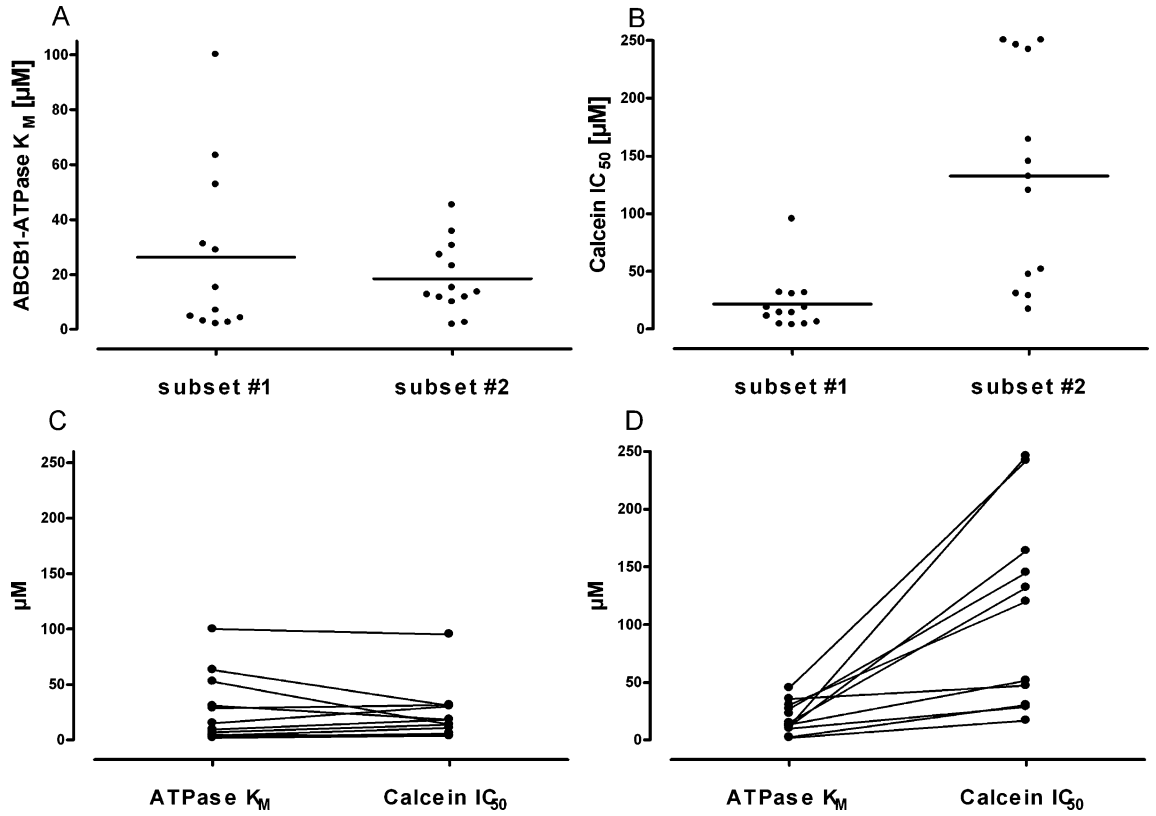

Fig. 6 Scatter plots of ABCB1-ATPase K_m values (**a**) and IC_{50} values for the inhibition of calcein AM efflux from K562-MDR1 cells (**b**) of validation compounds contained in subset 1 (high $P_{app\text{-}HDM}$) and subset 2 (low $P_{app\text{-}HDM}$). Comparison of ABCB1-ATPase K_m values and IC_{50} values for the inhibition of calcein AM for individual compounds contained in subset 1 (high $P_{app\text{-}HDM}$, **c**) and subset 2 (low $P_{app\text{-}HDM}$, **d**)

observed, whereas the permeability of none of the high $P_{app\text{-}HDM}$ compounds in subset 1 was affected by GF120918, indicating no effect of ABCB1 on the net flux of these compounds through Caco-2 cells (Fig. 7). The addition of 1 µM GF120918 increased the permeability coefficient of low passive permeability compounds in subset 2 on average 7.31-fold (range 1.45–24.2-fold), while no effect of the ABCB1 inhibitor was observed for the high permeability compounds contained in subset 1 (mean GF120198 ratio 1.06-fold, range 0.92–1.19-fold, cp. Table 2). In concert with the training set data, ABCB1-ATPase activity of validation set compounds, by itself, did not predict the effect of ABCB1 on compound permeability in the apical to basolateral direction (Fig. 5b).

Discussion

The substrate-binding site of ABCB1 is located within the plasma membrane or the cytoplasm (Ambudkar et al. 2005). Therefore, besides the affinity of a molecule to the substrate-binding site of ABCB1, the rate at which a molecule reaches this site from outside the plasma membrane governs the kinetics of ABCB1-mediated transport and inhibition (Bentz et al. 2005). The aim of this study was, therefore, to define and validate a rigorous, high-throughput screening procedure for assessing ABCB1 substrates and inhibitors by integrating passive permeability and ABCB1-ATPase activity.

The data on ABCB1-ATPase activity of compounds included in the training set known to interact with ABCB1 was found to be in concert with earlier reports (Garrigues et al. 2002b; Litman et al. 1997b). In order to fully appreciate the ABCB1-ATPase data presented in this study, an understanding of how ABCB1 couples ATP hydrolysis to drug transport is mandatory. Recent data indicate that ATP hydrolysis is an integral part in the transport cycle of ABCB1, since the formation of ABCB1 enzyme–substrate complexes is dependent on ATP hydrolysis (Sauna et al. 2006). However, when Eytan et al. (1996a) studied ABCB1-mediated uptake into inside-out membrane vesicles trapping an ionophore ($^{86}Rb^{+}$), the minimal substrate concentration required for stimulation of ABCB1-ATPase activity was higher than the concentration needed to observe appreciable ATP-dependent substrate uptake into membrane vesicles. It was speculated that the high basal activity demonstrated by ABCB1 presumably masked the ATPase activity required for ATP-dependent transport. In later

Table 2 ABCB1-ATPase activity, calcein AM, HDM-PAMPA, and Caco-2 data for validation set compounds (N=26)

No.	Compound	ATPase V_0/V_{max} (nmol/mg/min)	ATPase K_1 (μM)	ATPase type	Calcein assay IC_{50} (μM)	Calcein assay hill factor	P_{app} HDM-PAMPA ($cm \times 10^{-6}/s$)	Caco-2 P_{app} a–b ($cm \times 10^{-6}/s$)	Caco-2 P_{app} a–$b_{GF120918}$ ($cm \times 10^{-6}/s$)	Caco-2 GF120918 ratio[a]
1	BYK001	18.4/70.8	52.7	A	14.2	1.62	202	70.5	71.3	1.01
2	BYK002	10.2/35.2	6.96	A	14.0	1.45	98.9	71.8	74.3	1.03
3	BYK003	11.4/27.0	9.58	A	18.4	1.36	87.0	85.4	87.0	1.02
4	BYK004	13.8/74.6	31.0	A	18.4	1.53	68.2	82.5	82.0	0.99
5	BYK005	8.60/27.7	4.20	B	10.9	1.63	78.2	69.1	75.1	1.09
6	BYK006	14.5/70.0	63.3	A	31.3	2.24	33.5	65.1	77.7	1.19
7	BYK007	10.6/26.5	3.01	B	4.31	1.60	69.1	69.0	75.6	1.10
8	BYK008	15.4/70.7	4.69	A	3.61	1.22	89.2	77.4	71.1	0.92
9	BYK009	12.1/144	>100	A	95.3	0.90	56.5	68.0	78.1	1.15
10	BYK010	10.3/48.7	28.8	A	31.7	0.79	70.4	74.0	83.7	1.13
11	BYK011	9.65/27.4	2.07	B	4.23	1.47	85.9	73.8	78.2	1.06
12	BYK012	12.1/28.3	2.56	B	6.06	1.15	77.1	88.3	88.2	1.00
13	BYK013	9.40/22.7	15.2	A	30.5	0.95	51.1	82.0	88.9	1.08
14	BYK014	7.18/25.0	30.5	A	120	0.98	0.12	12.3	36.1	2.93
15	BYK015	14.7/40.8	15.1	A	132	1.25	0.18	5.88	17.8	3.03
16	BYK016	14.5/32.6	1.89	B	17.0	0.91	1.00	30.2	43.7	1.45
17	BYK017	9.49/30.7	13.6	A	51.6	0.67	0.42	15.3	26.8	1.75
18	BYK018	9.06/45.1	35.7	A	47.1	1.34	0.20	14.7	34.9	2.37
19	BYK019	11.7/44.7	27.1	A	145	2.08	0.03	3.44	6.23	1.81
20	BYK020	8.97/32.8	10.0	A	28.7	1.47	0.89	2.04	26.9	13.2
21	BYK021	10.1/20.9	12.7	A	No inhib.		0.09	0.76	4.47	5.88
22	BYK022	9.44/35.6	11.6	A	256	0.94	0.14	0.77	11.2	14.5
23	BYK023	8.52/39.5	45.2	A	252	1.43	0.16	0.26	6.30	24.2
24	BYK024	12.4/31.5	11.7	B	164	2.20	0.05	0.91	4.57	5.02
25	BYK025	13.3/35.8	2.45	B	30.6	1.64	0.41	0.89	14.1	15.8
26	BYK026	11.1/28.0	23.0	B	No inhib.		0.11	1.70	5.25	3.09

ABCB1-ATPase activity was categorized as follows: compounds that stimulate basal ABCB1-ATPase activity (type A), drugs that stimulate basal ABCB1-ATPase activity at low concentrations but inhibit the activity at higher concentrations (type B). ABCB1 inhibition was determined by measuring the inhibition of calcein AM efflux from K562-MDR cells. Permeability coefficients were determined through artificial hexadecane layers (HDM-PAMPA) and Caco-2 monolayers as described in the "Materials and methods" section

No inhib. compounds that did not inhibit calcein AM efflux from K562-MDR cells over the concentration range tested

[a] ABCB1 function, i.e., the effect of ABCB1 on the permeability of test compounds in the absorptive (apical to basolateral) direction expressed as the ratio of apparent permeability coefficients in the presence and absence of 1 μM GF120198

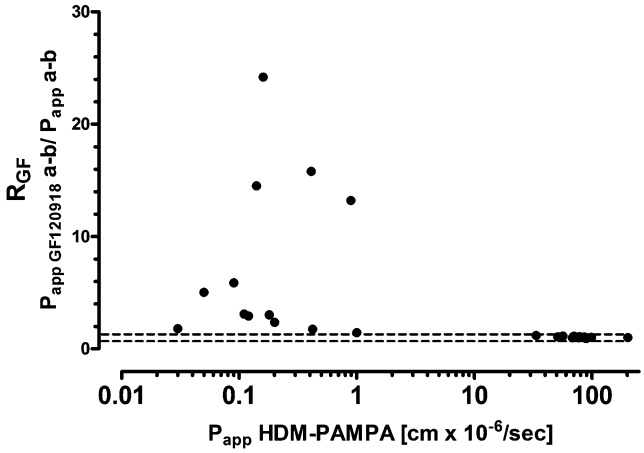

Fig. 7 Correlation between ABCB1 function determined as the ratio of apparent permeability across Caco-2 cells in the presence and absence of 1 μM GF120918 and passive permeability determined with HDM-PAMPA of validation set compounds. The *broken line* indicates the threshold ratios of 1.25 and 0.75 discriminating a compound that is actively transported. All compounds contained in the validation set were shown to stimulate ABCB1-ATPase activity

studies, it could be shown that this basal ABCB1-ATPase activity is tightly dependent on the presence of cholesterol in the membrane derived from Sf9 insect cells and that the stimulation of ABCB1-ATPase activity by ABCB1 substrates is higher in the absence than in the presence of cholesterol (Garrigues et al. 2002a). ABCB1-ATPase background activity in this study, i.e., the vanadate-sensitive ATPase activity measured in the DMSO controls in membrane fractions containing ABCB1, was low, i.e., on average 6.18±0.90 nmol P_i/mg/min (range 5.00 to 8.60 nmol P_i/mg/min), which is close to the ATPase activity in cholesterol-depleted MDR1-transfected Sf9 membrane fractions reported earlier (Garrigues et al. 2002a).

A possible explanation why cyclosporine A, fluvastatin, pumafentrine, and topotecan were not found to stimulate basal ABCB1-ATPase activity could be that the extent of stimulation is smaller than the basal ABCB1-ATPase activity conferred by endogenous substrates such as cholesterol. All four compounds, however, did inhibit verapamil-stimulated ABCB1-ATPase activity. The complex allosteric interplay between ABCB1 catalytic substrates and the protein reflected by its ATPase activity as well as the basal ATPase activity mediated by cholesterol or other membrane vesicle constituents are likely explanations for false-negative results obtained from ABCB1-ATPase data in earlier studies (Adachi et al. 2001). Furthermore, given the complex concentration–response relationship for ABCB1 ATPase observed in this study, the assessment of ABCB1 substrates using only single substrate concentrations is likely to produce false-negative results as described earlier (Polli et al. 2001). Using a combination of stimulation of basal ABCB1-ATPase activity and inhibition of verapamil-stimulated ABCB1-ATPase activity, we were able to identify all compounds that had previously been identified as ABCB1 substrates, either inhibiting the transporter or being actively transported in the cellular assays used. In a similar approach, using mdr1 prepared from Chinese hamster lung fibroblasts, Garrigues et al. (2002b) successfully identified 95% of ABCB1 substrates known from the literature when stimulation and inhibition of ABCB1-ATPase were combined.

In contrast to the localization of ABCB1 in the apical plasma membrane, ABCB1 function in cell monolayer assays is often assessed by determination of flux ratios, i.e., the ratio of secretory (basolateral–apical) over absorptive flux (apical–basolateral). However, there are several experimental constraints inherent to this approach such as different barrier properties, i.e., surface area, lipid composition of the apical and basolateral cell membrane in polarized epithelia reference (Le Grimellec et al. 1992). Furthermore, the secretory permeability comprises the transport of compounds through the basolateral followed by the apical plasma membrane, which can be biased by transporters localized in the basolateral membrane which has recently been demonstrated for digoxin (Acharya et al. 2008). In line with these considerations, it was recently shown that efflux ratios cannot assess ABCB1-mediated attenuation of absorptive transport in Caco-2 monolayer for a variety of ABCB1 substrates because of the asymmetric effect of the transporter on absorptive and secretory transport, suggesting the involvement of basolaterally directed transporters in the secretory transport of compounds such as etoposide and talinolol (Troutman and Thakker 2003a). We, therefore, chose to study ABCB1 function by comparing permeability coefficients of ABCB1 substrates in the apical to basolateral, i.e., absorptive, direction in Caco-2 cells in the presence and absence of the noncompetitive ABCB1 inhibitor GF120918.

ABCB1 function determined in Caco-2 cell monolayer was only apparent for training set compounds that exhibited low passive permeability coefficients ($P_{app\text{-}HDM}$ <2.0 cm× 10^{-6}/s). This finding is in line with earlier reports, suggesting that a net effect of ABCB1 on cellular accumulation can only occur when the efflux rate of the transporter surmounts the passive permeability rate of the substrate (Eytan 2005; Wu and Benet 2005). In contrast to the data presented in this study, cyclosporine A and quinidine absorptive transport under sink conditions defined as a compound flux of less than 10% were shown to be dependent on ABCB1 (Troutman and Thakker 2003b). It cannot be excluded that ABCB1 attenuates initial permeability rates of ABCB1 substrates that exhibit medium to high passive permeability coefficients. It has to be noted that we analyzed ABCB1 function under non-sink conditions applying a Caco-2 experimental setup commonly used

in compound screening, i.e., sampling one concentration at one time point (2 h). Using transcellular assays under sink conditions requires extensive sampling at multiple short time-intervals or the use of an Ussing chamber. Such experiments are usually limited to the availability of radiolabeled compounds in later stages of the drug development process (Troutman and Thakker 2003b). Moreover, the characterization of initial rate permeability across membrane bilayers requires real-time monitoring of compound flux (Eytan et al. 1996b) or sampling in the intervals of seconds that is difficult to adapt to transcellular assays. The data presented in this study, clearly indicate that ABCB1 function studied under non-sink conditions produces false-negative results. This finding is of pivotal importance for the ongoing discussion on the methodology to be used for identifying ABCB1 substrates: the recently published FDA recommendation on "Criteria for establishing whether an NME is a P-gp substrate and whether an in vivo interaction study is needed" (Huang et al. 2008) advocates the use of non-sink cellular models that, according to our data, could be prone to produce false-negative results for high permeability compounds. Therefore, the effect of ABCB1 on the initial rate permeability of highly permeable compounds requires further study.

In contrast to ABCB1 function, compounds that interacted with ABCB1-ATPase and displayed passive permeability coefficients greater than 2.0 $cm \times 10^{-6}$/s in the HDM-PAMPA assay did inhibit calcein AM efflux out of K562 MDR1 cells and were thus identified as ABCB1 inhibitors. The data indicate that, besides the affinity to ABCB1, the rate at which the substrate-binding sites can be accessed is an additional factor to be considered in the assessment of ABCB1 inhibition. Notably, passive permeability per se did not have an influence on ABCB1 substrate specificity because no correlation was found between the apparent K_m value of ABCB1-ATPase and passive permeability. Assuming that the ABCB1 substrate-binding site is on the cytosolic side of the plasma membrane, this finding can be explained, as the ABCB1 binding site that can be readily accessed in the inside-out membrane vesicles used for the ABCB-ATPase assay (Shapiro and Ling 1994).

Given the selection bias in the validation set for ABCB1 inhibitors, we subsequently tested the hypothesis that vanadate-sensitive ABCB1-ATPase activity can be successfully applied to identify ABCB1 substrates and inhibitors when combined with data on passive permeability. We analyzed a validation set consisting of 26 Altana Pharma compounds derived from different chemical series that all stimulated basal ABCB1-ATPase activity and were discriminated according to their passive permeability with high permeable compounds (subset 1: $P_{app\text{-}HDM} > 50$ $cm \times 10^{-6}$ cm/s) and low permeable compounds (subset 2: $P_{app\text{-}HDM} < 1$ $cm \times 10^{-6}$ cm/s). The results corroborated the effect of passive permeability as an important covariate of active transport: all high permeable compounds in subset 1 of the validation set did inhibit calcein AM efflux with a mean shift from ABCB1-ATPase K_m to IC_{50} for the inhibition of calcein AM efflux of 1.4-fold whereas the low passive permeability of compounds in subset 2 shifted the IC_{50} for the inhibition of calcein AM efflux by almost an order of magnitude. The data indicate that, for highly permeable compounds, the K_m value obtained from ABCB1-ATPase can be used to predict the IC_{50} value for the inhibition of calcein AM efflux within a twofold error for high permeable compounds assuming competitive inhibition. In contrast to ABCB1 inhibition, the transporter did not have an effect on the net flux on any of the high permeable compounds through the Caco-2 monolayer. Given the difference in passive permeability between the two subsets, the effect of passive permeability on ABCB1 function and inhibition was found to be more pronounced in the validation set than in the training set.

In conclusion, compounds that did not interact with vanadate-sensitive ABCB1-ATPase were not found to either inhibit the transporter or to be actively transported in the cellular assays used. The data presented in this study suggest classification of compounds that interact with ABCB1-ATPase into ABCB1-transported substrates and ABCB1 inhibitors based on passive permeability. The use of HDM-PAMPA in combination with ABCB1-ATPase offers a simple, inexpensive experimental approach capable of identifying ABCB1 substrates and inhibitors in a high-throughput fashion. Based on these data, compounds can be selected for subsequent in-depth analysis of ABCB1 inhibition and function in cellular assays carried out under initial rate conditions that demand longer assay times and higher cost.

Acknowledgements We are indebted to Silke Müller, Altana Pharma, Konstanz, Germany, for the excellent technical assistance in generating the Western blots. The authors are grateful to Dr. Michel Eichelbaum, Dr. Margarete Fischer-Bosch-Institute for Clinical Pharmacology, Stuttgart, Germany, for providing the human enterocytes. We would like to thank Dr. Bálazs Sarkadi, Budapest, Hungary and Dr. Geoff Tucker, Sheffield, UK for the fruitful and challenging discussion of the manuscript. Altana Pharma AG, Konstanz, Germany and Solvo Biotechnology, Budapest, Hungary supported this study. Work at Solvo Biotechnology was further supported by Hungarian Grants Asbóth KF208318/2005, GVOP-2004-3.3.2.-2004-04-0001/3.0, GVOP-3.1.1.-2004-05-0506/3.0, EEF-Munka 00034/2003, and European Community grants FP6-NoE005137, FP6-2004-LIFESCI-HEALTH-5; FP6-2004-LIFESCIHEALTH-5; Proposal No. 518246.

Conflict of interest statement Oliver von Richter, Stephanie Liehner, Beate Siewert, and Karl Zech are employees of Altana Pharma. Hristos Glavinas and Peter Krajcsi are employees of Solvo Biotechnology.

References

Acharya P, Tran TT, Polli JW, Ayrton A, Ellens H, Bentz J (2006) P-Glycoprotein (P-gp) expressed in a confluent monolayer of hMDR1-MDCKII cells has more than one efflux pathway with cooperative binding sites. Biochemistry 45:15505–15519

Acharya P, O'Connor MP, Polli JW, Ayrton A, Ellens H, Bentz J (2008) Kinetic identification of membrane transporters that assist P-glycoprotein-mediated transport of digoxin and loperamide through a confluent monolayer of MDCKII-hMDR1 cells. Drug Metab Dispos 36:452–460

Adachi Y, Suzuki H, Sugiyama Y (2001) Comparative studies on in vitro methods for evaluating in vivo function of MDR1 P-glycoprotein. Pharm Res 18:1660–1668

Allen JD, van Loevezijn A, Lakhai JM, van d V, van Tellingen O, Reid G, Schellens JH, Koomen GJ, Schinkel AH (2002) Potent and specific inhibition of the breast cancer resistance protein multidrug transporter in vitro and in mouse intestine by a novel analogue of fumitremorgin C. Mol Cancer Ther 1:417–425

Ambudkar SV, Lelong IH, Zhang J, Cardarelli CO, Gottesman MM, Pastan I (1992) Partial purification and reconstitution of the human multidrug-resistance pump: characterization of the drug-stimulatable ATP hydrolysis. Proc Natl Acad Sci USA 89:8472–8476

Ambudkar SV, Kim IW, Sauna ZE (2005) The power of the pump: mechanisms of action of P-glycoprotein (ABCB1). Eur J Pharm Sci 27:392–400

Balimane PV, Chong S (2005) Cell culture-based models for intestinal permeability: a critique. Drug Discov Today 10:335–343

Bentz J, Tran TT, Polli JW, Ayrton A, Ellens H (2005) The steady-state Michaelis–Menten analysis of P-glycoprotein mediated transport through a confluent cell monolayer cannot predict the correct Michaelis constant K_m. Pharm Res 22:1667–1677

Choo EF, Leake B, Wandel C, Imamura H, Wood AJ, Wilkinson GR, Kim RB (2000) Pharmacological inhibition of P-glycoprotein transport enhances the distribution of HIV-1 protease inhibitors into brain and testes. Drug Metab Dispos 28:655–660

Cordon-Cardo C, O'Brien JP, Casals D, Rittman-Grauer L, Biedler JL, Melamed MR, Bertino JR (1989) Multidrug-resistance gene (P-glycoprotein) is expressed by endothelial cells at blood-brain barrier sites. Proc Natl Acad Sci USA 86:695–698

Cummins CL, Jacobsen W, Benet LZ (2002) Unmasking the dynamic interplay between intestinal P-glycoprotein and CYP3A4. J Pharmacol Exp Ther 300:1036–1045

Drescher S, Glaeser H, Murdter T, Hitzl M, Eichelbaum M, Fromm MF (2003) P-glycoprotein-mediated intestinal and biliary digoxin transport in humans. Clin Pharmacol Ther 73:223–231

Essodaigui M, Broxterman HJ, Garnier-Suillerot A (1998) Kinetic analysis of calcein and calcein-acetoxymethylester efflux mediated by the multidrug resistance protein and P-glycoprotein. Biochemistry 37:2243–2250

Evers R, Kool M, van Deemter L, Janssen H, Calafat J, Oomen LC, Paulusma CC, Oude Elferink RP, Baas F, Schinkel AH, Borst P (1998) Drug export activity of the human canalicular multispecific organic anion transporter in polarized kidney MDCK cells expressing cMOAT (MRP2) cDNA. J Clin Invest 101:1310–1319

Evers R, Kool M, Smith AJ, van Deemter L, de Haas M, Borst P (2000) Inhibitory effect of the reversal agents V-104, GF120918 and Pluronic L61 on MDR1 Pgp-, MRP1- and MRP2-mediated transport. Br J Cancer 83:366–374

Eytan GD (2005) Mechanism of multidrug resistance in relation to passive membrane permeation. Biomed Pharmacother 59:90–97

Eytan GD, Regev R, Assaraf YG (1996a) Functional reconstitution of P-glycoprotein reveals an apparent near stoichiometric drug transport to ATP hydrolysis. J Biol Chem 271:3172–3178

Eytan GD, Regev R, Oren G, Assaraf YG (1996b) The role of passive transbilayer drug movement in multidrug resistance and its modulation. J Biol Chem 271:12897–12902

Fromm MF (2004) Importance of P-glycoprotein at blood-tissue barriers. Trends Pharmacol Sci 25:423–429

Garrigues A, Escargueil AE, Orlowski S (2002a) The multidrug transporter, P-glycoprotein, actively mediates cholesterol redistribution in the cell membrane. Proc Natl Acad Sci USA 99:10347–10352

Garrigues A, Nugier J, Orlowski S, Ezan E (2002b) A high-throughput screening microplate test for the interaction of drugs with P-glycoprotein. Anal Biochem 305:106–114

Glavinas H, Krajcsi P, Cserepes J, Sarkadi B (2004) The role of ABC transporters in drug resistance, metabolism and toxicity. Curr Drug Deliv 1:27–42

Goh LB, Spears KJ, Yao D, Ayrton A, Morgan P, Roland WC, Friedberg T (2002) Endogenous drug transporters in in vitro and in vivo models for the prediction of drug disposition in man. Biochem Pharmacol 64:1569–1578

Greiner B, Eichelbaum M, Fritz P, Kreichgauer HP, von Richter O, Zundler J, Kroemer HK (1999) The role of intestinal P-glycoprotein in the interaction of digoxin and rifampin. J Clin Invest 104:147–153

Homolya L, Hollo M, Muller M, Mechetner EB, Sarkadi B (1996) A new method for a quantitative assessment of P-glycoprotein-related multidrug resistance in tumour cells. Br J Cancer 73:849–855

Huang SM, Strong JM, Zhang L, Reynolds KS, Nallani S, Temple R, Abraham S, Habet SA, Baweja RK, Burckart GJ, Chung S, Colangelo P, Frucht D, Green MD, Hepp P, Karnaukhova E, Ko HS, Lee JI, Marroum PJ, Norden JM, Qiu W, Rahman A, Sobel S, Stifano T, Thummel K, Wei XX, Yasuda S, Zheng JH, Zhao H, Lesko LJ (2008) New era in drug interaction evaluation: US Food and Drug Administration update on CYP enzymes, transporters, and the guidance process. J Clin Pharmacol 48:662–670

Klimecki WT, Futscher BW, Grogan TM, Dalton WS (1994) P-glycoprotein expression and function in circulating blood cells from normal volunteers. Blood 83:2451–2458

Kruijtzer CM, Beijnen JH, Rosing H, Bokkel Huinink WW, Schot M, Jewell RC, Paul EM, Schellens JH (2002) Increased oral bioavailability of topotecan in combination with the breast cancer resistance protein and P-glycoprotein inhibitor GF120918. J Clin Oncol 20:2943–2950

Le Grimellec C, Friedlander G, el Yandouzi EH, Zlatkine P, Giocondi MC (1992) Membrane fluidity and transport properties in epithelia. Kidney Int 42:825–836

Litman T, Nielsen D, Skovsgaard T, Zeuthen T, Stein WD (1997a) ATPase activity of P-glycoprotein related to emergence of drug resistance in Ehrlich ascites tumor cell lines. Biochim Biophys Acta 1361:147–158

Litman T, Zeuthen T, Skovsgaard T, Stein WD (1997b) Structure-activity relationships of P-glycoprotein interacting drugs: kinetic characterization of their effects on ATPase activity. Biochim Biophys Acta 1361:159–168

Martin C, Berridge G, Higgins CF, Mistry P, Charlton P, Callaghan R (2000) Communication between multiple drug binding sites on P-glycoprotein. Mol Pharmacol 58:624–632

Meissner K, Sperker B, Karsten C, Zu Schwabedissen HM, Seeland U, Bohm M, Bien S, Dazert P, Kunert-Keil C, Vogelgesang S, Warzok R, Siegmund W, Cascorbi I, Wendt M, Kroemer HK (2002) Expression and localization of P-glycoprotein in human heart: effects of cardiomyopathy. J Histochem Cytochem 50:1351–1356

Nielsen PE, Avdeef A (2004) PAMPA—a drug absorption in vitro model 8. Apparent filter porosity and the unstirred water layer. Eur J Pharm Sci 22:33–41

Petzinger E, Burckhardt G, Tampe R (2006) A multi-faceted world of transporters. Naunyn-Schmiedeberg's Arch Pharmacol 372:383–384

Polli JW, Wring SA, Humphreys JE, Huang L, Morgan JB, Webster LO, Serabjit-Singh CS (2001) Rational use of in vitro P-glycoprotein assays in drug discovery. J Pharmacol Exp Ther 299:620–628

Sarkadi B, Price EM, Boucher RC, Germann UA, Scarborough GA (1992) Expression of the human multidrug resistance cDNA in insect cells generates a high activity drug-stimulated membrane ATPase. J Biol Chem 267:4854–4858

Sauna ZE, Nandigama K, Ambudkar SV (2006) Exploiting reaction intermediates of the ATPase reaction to elucidate the mechanism of transport by P-glycoprotein (ABCB1). J Biol Chem 281:26501–26511

Shapiro AB, Ling V (1994) ATPase activity of purified and reconstituted P-glycoprotein from Chinese hamster ovary cells. J Biol Chem 269:3745–3754

Smit JW, Huisman MT, van Tellingen O, Wiltshire HR, Schinkel AH (1999) Absence or pharmacological blocking of placental P-glycoprotein profoundly increases fetal drug exposure. J Clin Invest 104:1441–1447

Thiebaut F, Tsuruo T, Hamada H, Gottesman MM, Pastan I, Willingham MC (1987) Cellular localization of the multidrug-resistance gene product P-glycoprotein in normal human tissues. Proc Natl Acad Sci USA 84:7735–7738

Troutman MD, Thakker DR (2003a) Efflux ratio cannot assess P-glycoprotein-mediated attenuation of absorptive transport: asymmetric effect of P-glycoprotein on absorptive and secretory transport across Caco-2 cell monolayers. Pharm Res 20:1200–1209

Troutman MD, Thakker DR (2003b) Novel experimental parameters to quantify the modulation of absorptive and secretory transport of compounds by P-glycoprotein in cell culture models of intestinal epithelium. Pharm Res 20:1210–1224

von Richter O, Burk O, Fromm MF, Thon KP, Eichelbaum M, Kivisto KT (2004) Cytochrome P450 3A4 and P-glycoprotein expression in human small intestinal enterocytes and hepatocytes: a comparative analysis in paired tissue specimens. Clin Pharmacol Ther 75:172–183

Wohnsland F, Faller B (2001) High-throughput permeability pH profile and high-throughput alkane/water log P with artificial membranes. J Med Chem 44:923–930

Wu CY, Benet LZ (2005) Predicting drug disposition via application of BCS: transport/absorption/elimination interplay and development of a biopharmaceutics drug disposition classification system. Pharm Res 22:11–23

Yee S (1997) In vitro permeability across Caco-2 cells (colonic) can predict in vivo (small intestinal) absorption in man—fact or myth. Pharm Res 14:763–766

Zhang JH, Chung TD, Oldenburg KR (1999) A simple statistical parameter for use in evaluation and validation of high throughput screening assays. J Biomol Screen 4:67–73